



GLOBAL JOURNAL OF SCIENCE FRONTIER RESEARCH: A  
PHYSICS AND SPACE SCIENCE  
Volume 16 Issue 1 Version 1.0 Year 2016  
Type : Double Blind Peer Reviewed International Research Journal  
Publisher: Global Journals Inc. (USA)  
Online ISSN: 2249-4626 | Print ISSN: 0975-5896 | DOI: 10.17406

# Dielectric and Radiative Properties of Surface Water over the Persian Gulf at L-Band

By Ali Rezaei - Latifi

*Hormozgan University*

**Abstract-** For microwave remote sensing applications over the ocean using radars and radiometers, a precise knowledge of dielectric and radiative Properties of surface water is required. In present work, spatial and temporal variability of the complex permittivity and refractive index, as well as reflectivity of Persian Gulf water for normal incidence, at L-Band (1.4 GHz), which has not been investigated before, is studied by using an empirical model. The calculations results indicate a relatively significant spatial and seasonal variability in the dielectric and radiative properties of the Gulf due to large variations in temperature and salinity of surface water. The mean real refractive index  $n$  over the Gulf surface water varies from a minimum value of 7.295 in December to a maximum value of 7.875 in June with annual mean of 7.581. The extinction coefficient  $k$  reaches maximum value of 2.036 in June and minimum value of 1/303 in January and its annual mean over the Persian Gulf is 1.674.

**Keywords:** *permittivity, refractive index, reflectivity, persian gulf, L-band.*

**GJSFR-A Classification :** FOR Code: 029999p



*Strictly as per the compliance and regulations of :*



# Dielectric and Radiative Properties of surface Water over the Persian Gulf at L-Band

Ali Rezaei - Latifi

**Abstract-** For microwave remote sensing applications over the ocean using radars and radiometers, a precise knowledge of dielectric and radiative Properties of surface water is required. In present work, spatial and temporal variability of the complex permittivity and refractive index, as well as reflectivity of Persian Gulf water for normal incidence, at L-Band (1.4 GHz), which has not been investigated before, is studied by using an empirical model. The calculations results indicate a relatively significant spatial and seasonal variability in the dielectric and radiative properties of the Gulf due to large variations in temperature and salinity of surface water. The mean real refractive index  $n$  over the Gulf surface water varies from a minimum value of 7.295 in December to a maximum value of 7.875 in June with annual mean of 7.581. The extinction coefficient  $k$  reaches maximum value of 2.036 in June and minimum value of 1/303 in January and its annual mean over the Persian Gulf is 1.674.

**Keywords:** permittivity, refractive index, reflectivity, persian gulf, L-band.

## 1. INTRODUCTION

Knowledge of dielectric properties of water is essential for calculating the radiative transfer coefficient of microwave radiation that is emitted by the ocean surface. Basis for the dielectric properties of a medium is its complex relative permittivity. Permittivity determines such intrinsic characteristics of the medium as skin (and penetration) depth, impedance, refractive index, etc. These quantities control the attenuation due to absorption and scattering and the transmission and reflection of the electromagnetic (EM) radiation in the medium. These radiative processes affect, in turn, the energy lost in and then emitted by the medium (Magdalena and Peter 2012). The real part of permittivity is known as the dielectric constant  $\epsilon'$  and is a measure of the ability of a material to be polarized and store energy. The imaginary part  $\epsilon''$  is a measure of the ability of the material to dissipate stored energy into heat.

Permittivity models for the permittivity of aqueous saline solutions and seawater given by Klien and Swift (1997), Stogryn (1971), Ellison et al. (1998), Meissner & Wenz (2004) and Blanch & Aguiasca (2004) were studied. These models provide the relative permittivity and conductivity of seawater at particular

microwave frequency as a function of the salinity and temperature. These models are based upon experimental data, performed by respective authors as well as the laboratory data others. The experimental data were fitted to empirical and theoretical expressions for calculation of relative permittivity of seawater for any frequency, salinity and temperature value desired. The Klien and swift (K&S) model is widely used for seawater dielectric coefficients. Comparison of measurement results with this model shows that real part is well in agreement. However, the experimental loss factor is slightly higher compared with the theoretical model (Joshi et al. 2012, Lang et al. 2003). Comparison between Blanch & Aguiasca(B&A) model with the other existing ones, on the other hand, showed that B&A model is close to the K& B model for the real part of permittivity and a bit high absolute values for imaginary part than the K&S model. Therefore the B&A model appears to be more accurate than well-known model of K&S.

The Persian Gulf is an important military, economic and political region owing to its oil and gas resources and is one of the busiest waterways in the world. Countries bordering the Persian Gulf are the United Arab Emirates(UAE), Saudi Arabia, Qatar, Bahrain, Kuwait and Iraq on one side and Iran on the other side (Fig. 1). The average depth of the Gulf is 36 m. Extensive shallow regions, <20m deep, are found along the coast of United Arab Emirates, around Bahrain, and at the head of the Gulf. Deeper portions, >40m deep, are found along the Iranian coast continuing into the Strait of Hormuz, which has a width of ~56 km and connects the Persian Gulf via the Gulf of Oman with the northern Indian Ocean (Kampf and Sadrinassab 2006). The Persian Gulf is one of the most saline water masses in world ocean and due to its shallow nature and sub-tropical climate both the salinity and temperature experiences dramatic spatial and temporal variations (Hassanzadeh et al 2011, Hosseinibalam et al. 2011).

*Author:* Hormozgan University. e-mail: r\_latifi@hormozgan.ac.ir

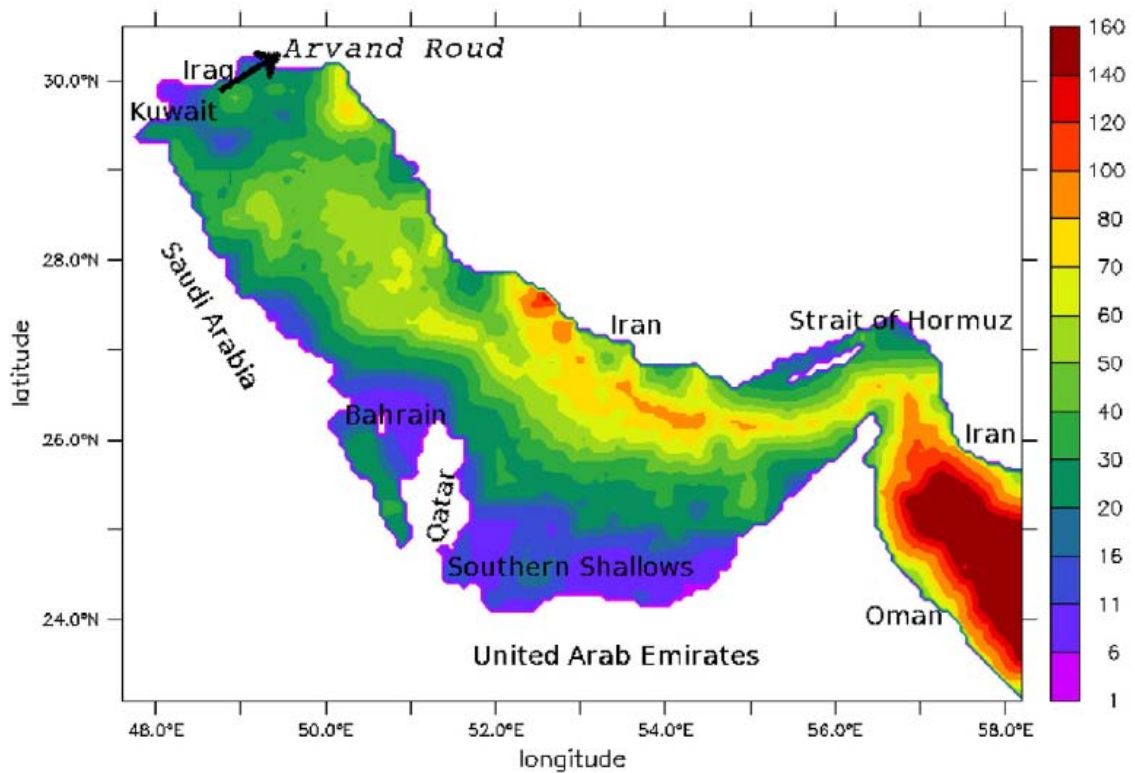


Fig. 1: Bathymetry and map of the Persian Gulf

In this work, spatial and seasonal variability of the complex permittivity and refractive index of Persian Gulf water in the long wavelength end of the microwave spectrum (1.4 GHz, L-band), is investigated by using empirical model of B&A. The salinity and temperature data of Persian Gulf water are required in order to calculate the relative permittivity and refractive index. Unfortunately, field data of salinity and temperature in the Persian Gulf are scarce and sparse. Thus, we use numerical data obtained from our previous work for estimation of permittivity. These data are in a relatively good agreement with limited direct measurements in the Persian Gulf (Hassanzadeh et al. 2011, Hosseinibalam et al. 2011, Hassanzadeh et al. 2012).

The outline of this paper is as follows. In section 2 the permittivity model reported by Blanch and Aguiasca and the formulas required to estimate the refractive index is presented. The results of calculation of parts of real and imaginary of permittivity and refractive index over the Persian Gulf are analyzed in section 3. The last section provides the conclusion.

## II. MATERIALS AND METHODS

As mentioned earlier, In order to calculate the complex permittivity are required the salinity and temperature data. We previously simulated these data by using a 3-dimensional numerical model. The model is based on hydrostatic versions of the Navier-Stokes equations that embrace conservation equations for momentum, volume, heat and salt. See our previous

works for details on how to set up and run the numerical model Gulf (Hassanzadeh et al. 2011, Hosseinibalam et al. 2011, Hassanzadeh et al. 2012). The Blanch and Aguiasca (2004) model, which is used to compute the complex permittivity together with formulas of refractive index are described as follows.

### a) Blanch and Aguiasca model

The dielectric properties of the liquids described by the Debye model (1926).

$$\hat{\epsilon} = \epsilon' - j\epsilon'' = \epsilon_{\infty} + \frac{\epsilon_s - \epsilon_{\infty}}{1 + j\omega\tau} - j \frac{\sigma}{\omega\epsilon_0} \quad (1-2)$$

Where  $\epsilon_{\infty}$  is the permittivity at optical frequencies,  $\epsilon_s$  is the static permittivity,  $\tau$  is the relaxation time and  $\sigma$  the ionic conductivity. The value of  $\epsilon_{\infty}$  is assumed to be constant, independent of salinity and temperature (its exact value is not critical in L-narrowband,  $0.5\text{GHz} \leq \nu \leq 2.5\text{GHz}$ ) and equal to 4.9. The  $\epsilon_s$  and  $\tau$  are both modeled as product of the values for distilled water and a term that depends on temperature (T) and salinity (S):

$$\begin{aligned} \epsilon_s(T, S) &= \epsilon_s(T, 0).a(T, S) \\ \tau(T, S) &= \tau(T, 0).b(T, S) \end{aligned} \quad (2-2)$$

The conductivity follows an exponential law.

$$\sigma(T, S) = \sigma(25, S).e^{-\phi} \quad (3-2)$$

According to the above equations, the seawater permittivity is a function of frequency, temperature and salinity. Blanch and Aguasca (2004) performed a lot of measurements in wide range of values those

parameters in order to obtain the coefficients of the permittivity model. Final results in  $0.5GHZ \leq \nu \leq 2.5GHZ$  are:

$$\epsilon_s(T,0) = 87.38 - 3.436 \times 10^{-1}T - 1.912 \times 10^{-3}T^2 + 3.812 \times 10^{-5}T^3 \tag{4-2}$$

$$a(T,S) = 1 + 1.1552 \times 10^{-5}TS - 3.9073 \times 10^{-3}S + 3.0596 \times 10^{-5}S^2 \tag{5-2}$$

$$\tau(T,0) = 17.385 - 5.78 \times 10^{-1}T + 1.084 \times 10^{-2}T^2 - 9.098 \times 10^{-5}T^3 \quad ps \tag{6-2}$$

$$b(T,S) = 1 + 2.9832 \times 10^{-4}TS - 2.3871 \times 10^{-3}S + 5.625 \times 10^{-5}S^2 \tag{7-2}$$

$$\sigma(25,S) = 1.90 \times 10^{-1}S - 2.35 \times 10^{-3}S^2 + 3.46 \times 10^{-5}S^3 \tag{8-2}$$

$$\phi = \Delta[1.9479 \times 10^{-2} + 1.6532 \times 10^{-4}\Delta - S(-1.0024 \times 10^{-6} + 6.9946 \times 10^{-7}\Delta)] \tag{9-2}$$

Where

$$\Delta = 25 - T \tag{10-2}$$

It should be noted that according to equation (1-2) the real and imaginary parts of the relative permittivity are as follows:

$$\epsilon' = \epsilon_\infty(T,S) + \frac{\epsilon_s(T,S) - \epsilon_\infty(T,S)}{1 + 4\pi^2\nu^2\tau^2(T,S)} \tag{11-2}$$

$$\epsilon''(\nu,T,S) = \frac{(\epsilon_s(T,S) - \epsilon_\infty(T,S))2\pi\nu\tau(T,S)}{1 + 4\pi^2\nu^2\tau^2(T,S)} + \frac{\sigma(T,S)}{2\pi\nu\epsilon_0} \tag{12-2}$$

b) *Complex refractive index*

The refractive index of a material is the factor that relates the phase velocity of electromagnetic radiation in that material, relative to its velocity in another medium or material. The absolute refractive index is relative to the velocity of light in the vacuum. The refractive index is a complex value,  $\hat{n} = n - jk$ . Here the real part  $n$  is the refractive index indicating the phase velocity as above, while the imaginary part  $k$  is called the extinction coefficient, which indicates the amount of absorption loss when the electromagnetic wave propagates through the material ( $j = \sqrt{-1}$ ).

The complex refractive index  $\hat{n} = n - jk$  and complex relative permittivity  $\hat{\epsilon} = \epsilon' - j\epsilon''$  are related following relation (John et al. 2008):

$$\hat{\epsilon} = \hat{n}^2 \tag{13-2}$$

By equating the real and imaginary parts we get:

$$\epsilon' = n^2 - k^2 \tag{14-2}$$

$$\epsilon'' = 2nk \tag{15-2}$$

These equations can be solved for  $n$  and  $k$ :

$$n = \left(\frac{\epsilon'}{2}\right)^{1/2} \left\{ \left[ 1 + \left(\frac{\epsilon''}{\epsilon'}\right)^2 \right]^{1/2} + 1 \right\}^{1/2} \tag{16-2}$$

$$k = \left(\frac{\epsilon'}{2}\right)^{1/2} \left\{ \left[ 1 + \left(\frac{\epsilon''}{\epsilon'}\right)^2 \right]^{1/2} - 1 \right\}^{1/2} \tag{17-2}$$

In addition, for normal incidence, the reflectivity is given by

$$r = \frac{(n-1)^2 + k^2}{(n+1)^2 + k^2} \tag{18-2}$$

For reflection at angles of incidence other than normal incidence, the reflection coefficient depends on the polarization of the electric field relative to surface.

### III. RESULTS

a) *Variability of the relative permittivity*

The calculations results indicate a significant spatial and temporal variability in the dielectric constant  $\epsilon'$  and dielectric loss  $\epsilon''$  of the Persian Gulf at L-band (1.4 GHZ) due to large seasonal variations in temperature and salinity of surface water. The mean dielectric constant attains a minimum and maximum value during the summer and winter respectively, and varies from 68.18 in June to 71.81 in late January (Fig2 and table 1).

The dielectric loss  $\epsilon''$  varies from 73.85 in January to 93.44 in June (table 1). Dielectric loss temporal variability of Persian Gulf water is stronger than dielectric constant and it gets maximum values in June-August and minimum values in months of December-January (Fig. 3). The comparison between figures 2 and 3 shows that an inverse relationship exists between real and imaginary parts of permittivity so that when one of two increases, the other variable decreases, and vice versa. In addition, analyses of obtained results indicate in L-

band the dielectric constant of the Persian Gulf water usually decreases with increase in salinity, whereas the dielectric loss of water increases with increase in salinity. Conversely, the dielectric constant goes higher to lower value and dielectric loss lower to higher with increase in the values of temperature. These results are in agreement with previous theoretical and experimental researches (Blanch and Aguiasca 2004, Joshi et al. 2012, Gadani et al. 2012).

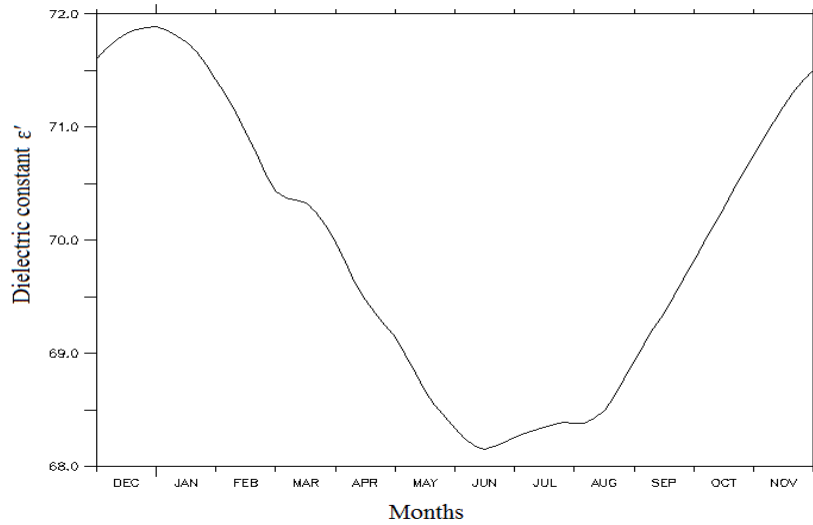


Fig. 2: Time series of domain-averaged dielectric constant  $\epsilon'$  at L-band

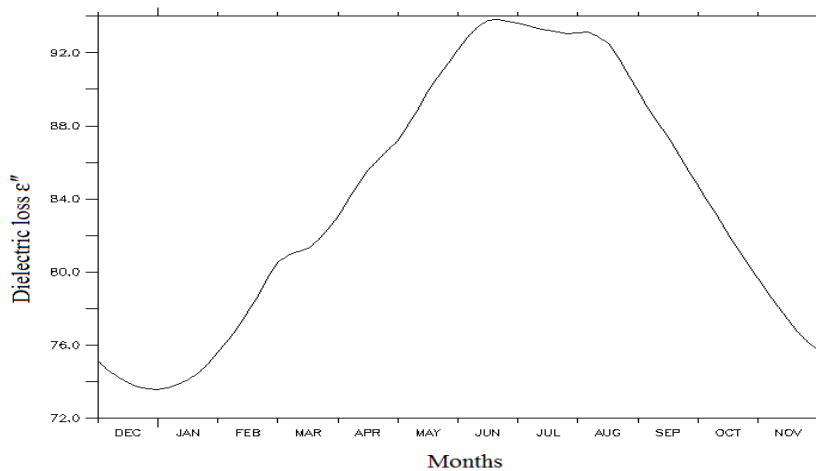


Fig. 3: Time series of domain-averaged dielectric loss  $\epsilon''$  at L-band

**Table 1:** Monthly surface mean of Dielectri constant  $\epsilon'$ , dielectric loss  $\epsilon''$ , real refractive index n, extinction coefficient k, Temperature T and salinity S of the Persian Gulf

Month	$\epsilon'$	$\epsilon''$	n	k	T	S
December	71.77	74.25	7.306	1.315	19.47	38.83
January	71.78	73.85	7.295	1.303	19.43	38.65
February	71.73	76.98	7.377	1.413	21.91	38.61
March	70.36	81.11	7.493	1.562	24.59	38.82
April	69.62	84.79	7.601	1.667	27.22	38.91
May	68.82	88.97	7.729	1.863	30.14	38.97
June	68.18	93.44	7.875	2.036	32.34	39.51
July	68.32	93.35	7.873	2.028	31.70	39.84
August	68.43	92.91	7.859	2.010	31.28	39.91
September	69.22	88.16	7.707	1.824	28.42	39.65
October	70.13	82.96	7.549	1.627	24.69	39.33
November	71.04	78.10	7.410	1.450	22.03	39.09

The salinity and temperature of Persian Gulf water significantly change due to factors such as inflow seasonal variations of low- salinity surface water of Indian Ocean (<37) into the Gulf through the Hormuz Strait, the seasonal changes in the weather and the turbulence mixing processes (figs. 4,5 and table 1). Gulf-averaged temperature follows the seasonal cycle of incident solar radiation and it attains its minimum and maximum values in months of December- January and June- August, respectively (Fig. 5). Gulf-averaged salinity, on the other hand, attains minimum values during January-March and maximum values June-August each year (Fig. 4). In general, Surface water of Persian Gulf is saltier in autumn and early winter than spring. In addition, the field and numerical studies indicate that salinity over the northeast areas in winter is saltier than spring and early summer (Hasanzadeh et al. 2011, Swift and Bower 2003). A Main reason for this unusual phenomenon is inflow increase of low- salinity

surface water of Indian Ocean (<37) into the Gulf through the Hormuz Strait over the months of spring and summer due to increase in evaporation rate, and a significant reduction of inflow in autumn. The other reason is the action of lateral and vertical mixing eddies generated by the wind forcing and thermohaline fluxes in winter and autumn. during spring and summer, the density is strongly stratified and established a vertically baroclinic stability in the Gulf, mainly as are sult of the strong surface heating. In winter and autumn, together with a weakening density contrast, under the influence the atmospheric cooling, the turbulence mixing processes in the Gulf occur and rapidly deepen the surface mixed layer. Since lower layers are saltier than surface water, the deepening of the mixed layer leads to an increase in the salinity of the surface. Effects of precipitation and river run-off on salinity changes are negligible on a Gulf-wide scale.

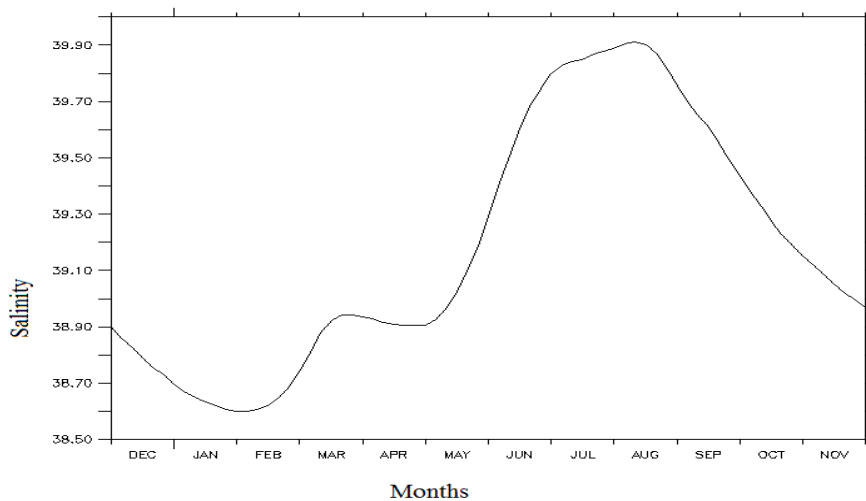


**Fig. 4:** Time series of domain-averaged salinity over the Persian Gulf

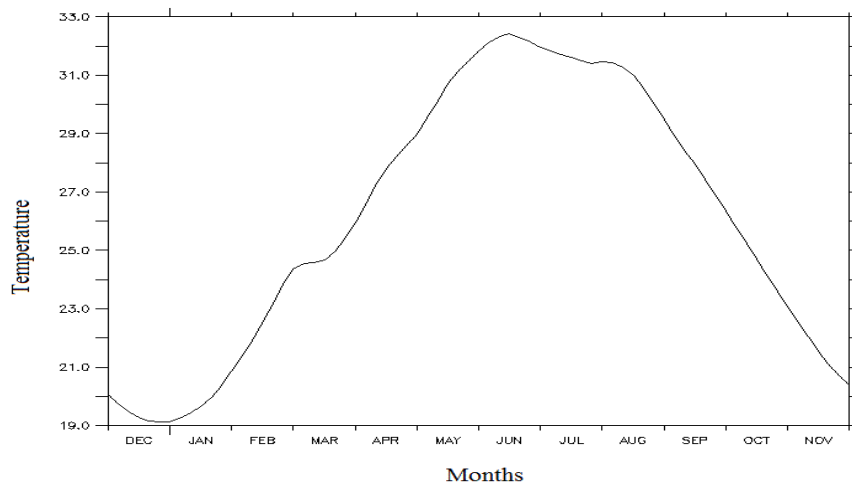


*Fig. 5:* Time series of domain-averaged temperature over the Persian Gulf

Fig. 6 indicates spatial distribution of dielectric constant in the middle of each season. In winter, spatial distribution of dielectric constant is weaker than the other seasons due to of lateral and vertical mixing eddies generated by the wind and thermohaline forcing. In spring and summer, increasing the weather temperature the static stability of water increases as a result, the lateral stratification is reinforced and dielectric constant gradually decreases from Iran coasts toward southern shallow regions. In autumn, this regular stratification relatively decreases under the action of mesoscale eddies that start to form in this season. with the exception of small area in the northern end, both Minimum and maximum dielectric constant with values of 68 and 72.2, usually are found over southern shallow regions along the UAE and Bahrain coasts in summer and winter, respectively. This is mainly due to shallow nature and large temperature difference of 16°C between summer and winter in these regions.



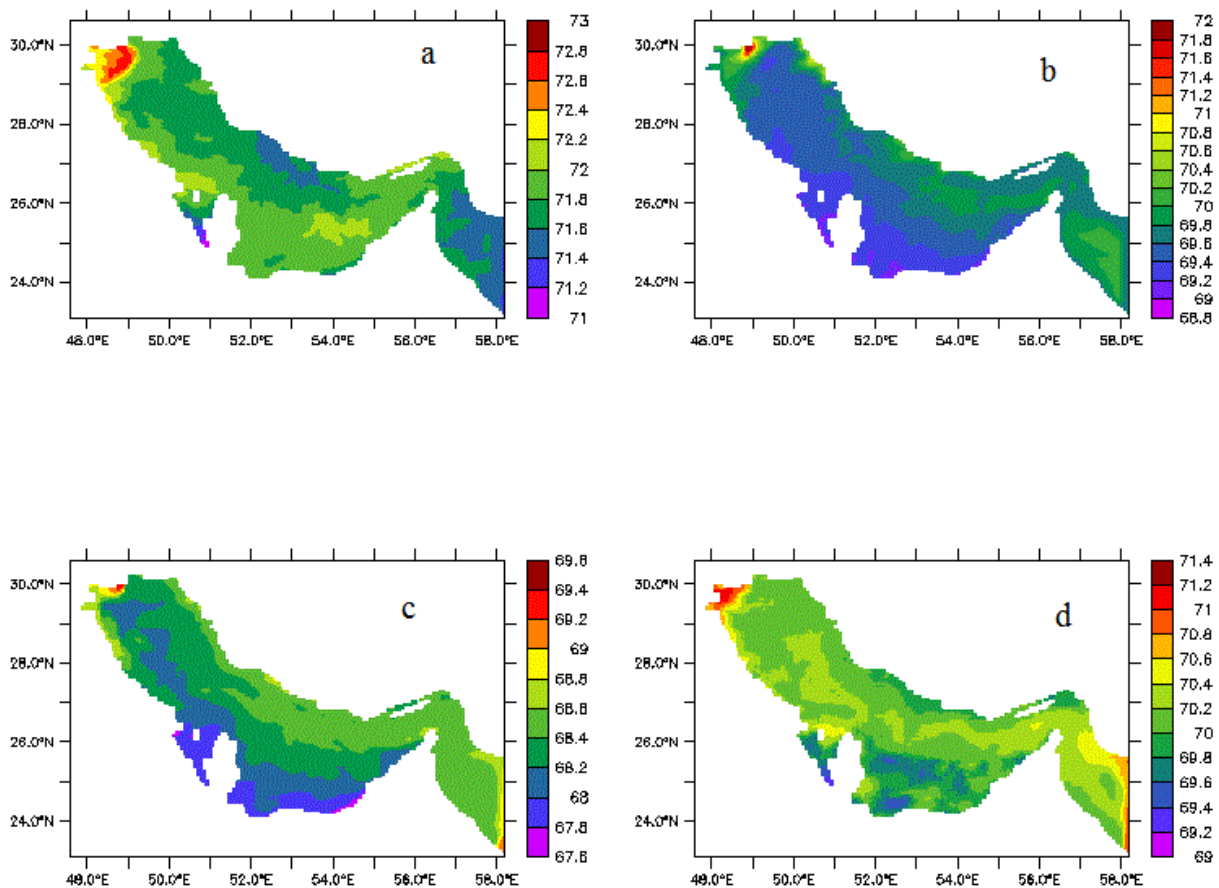


Fig. 6: The surface dielectric constant at L-band on (a) January 15, (b) April 15, (c) July 15 and (d) October 15

Spatial variability of dielectric loss at L-band is shown in fig. 7. Contrary to dielectric constant, the dielectric loss decreases from southern shallow parts to northeast deep regions. Spatial distribution of imaginary part of permittivity is to some extent uniform and varies about 72-74 over most parts of the Gulf in winter. With the exception of small area at the northwest end and south, almost a two-layer structure of dielectric loss is formed at most areas of the Gulf in Spring, with value of 80-85 within northeast regions and 85-90 over the other places of the Gulf. spatial variability in summer is stronger than the other seasons so that loss difference between southern and northeast areas reach about 20 on July 15. Main reasons for this relatively strong stratification are significant increase of salinity and temperature over the shallow regions and increase of low-salinity in flow from Hormuz Strait toward Iran coasts (Hasanzadeh et al. 2011, Swift and Bower 2003). In autumn, under the effects of lateral stirring of mesoscale eddies and convective deepening of the surface mixed layer the lateral contrast of dielectric loss is weakened and its value in most areas of gulf is about 82-86.



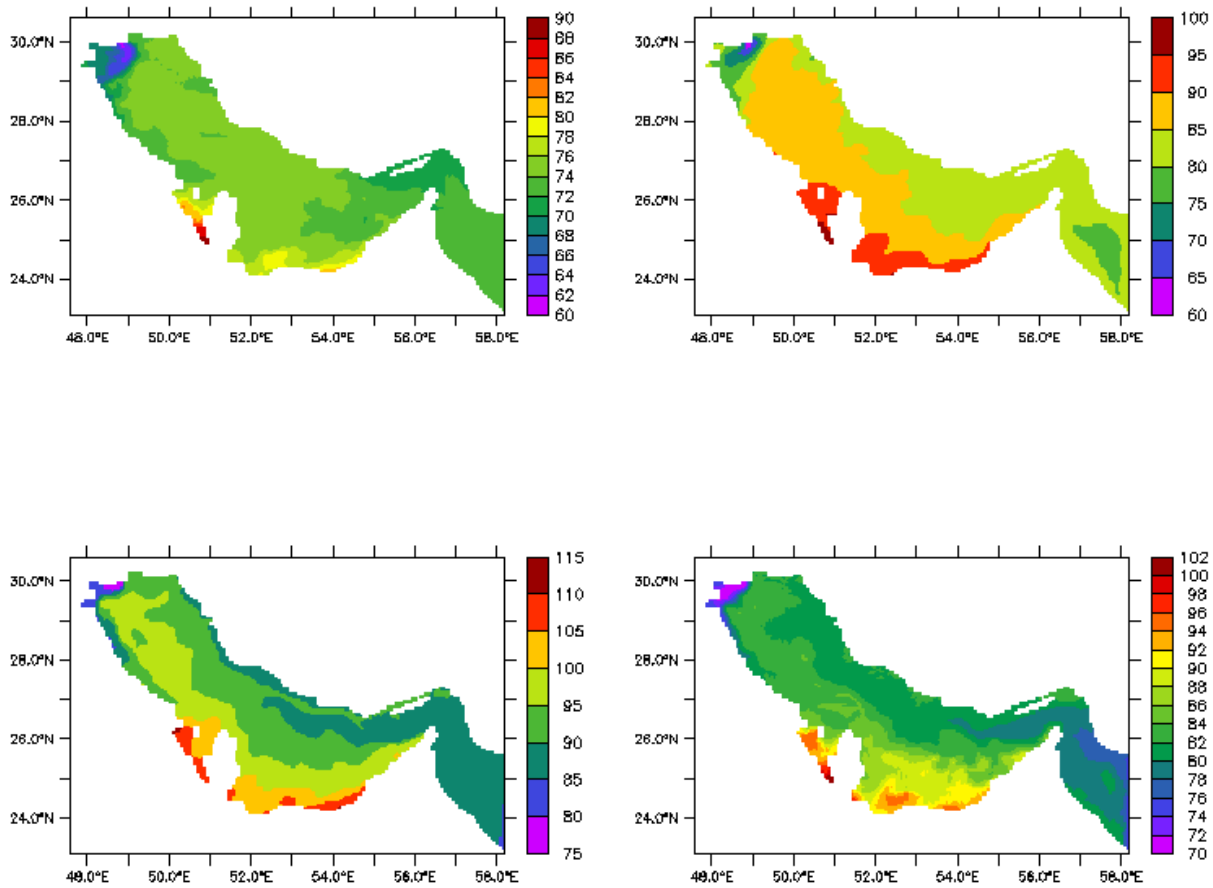


Fig. 7: The surface dielectric loss at L-band on (a) January 15, (b) April 15, (c) July 15 and (d) October 15

b) Variability of the refractive index

The domain-averaged of real refractive index  $n$  over the Gulf surface water varies from minimum value of 7.295 in December to maximum value of 7.875 in June (Fig.8 and table 1). The annual mean of basin-averaged is 7.581 at L-band. The highest rate of temporal variation of  $n$  is related to the spring months and its variability in summer months is relatively weak. Temporal variability of basin-averaged of imaginary refractive index  $k$  to a large extent qualitatively is similar to its counterpart  $n$  and as the real refractive index  $n$ , its variation rate is faster in spring (Fig. 9). This rapid changes in complex permittivity and refractive index in spring mainly related to a temperature increase of more than  $6^{\circ}\text{C}$  from March to June. The imaginary refractive index reach maximum value of 2.036 in June and minimum value of 1/303 in January and its annual mean over the Persian Gulf is 1.674.

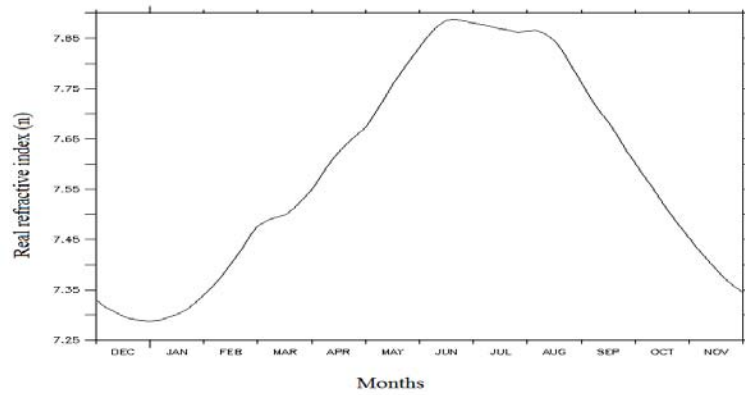


Fig. 8: Time series of domain-averaged of the real part of complex refractive index  $n$  at the Persian Gulf

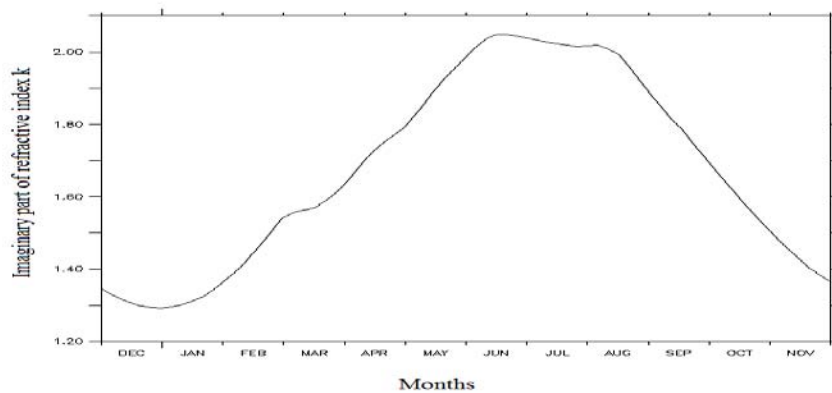


Fig. 9: Time series of domain-averaged of the imaginary part of complex refractive index  $k$  over the Persian Gulf

Figures 10 and 11 show spatial variability of parts of real and imaginary refractive index over the Gulf. In mid-winter the complex refractive index of surface water is relatively uniform and its real and imaginary parts have values of 7.3 and 1.3 respectively, at most areas of the Gulf. In mid-spring, both real and imaginary part of the refractive index from northern deep regions toward southern shallow regions increases by 0.5. The spatial distribution of real and imaginary of refractive index in mid-summer is almost similar to mid-spring but they both increase about 0.3-0.5. In autumn, over narrow region along the Iran coast real refractive index is about 7.4 and in other places with the exception southern shallow near at the UAE is about 7.6. In addition, at Iranian half of the Gulf the extinction coefficient  $k$  is about 1.4 and at other regions varies from 1.7 to 2.1 in this season. Totally, temporal variability the complex refractive index over shallow regions of Gulf is more than deep regions.

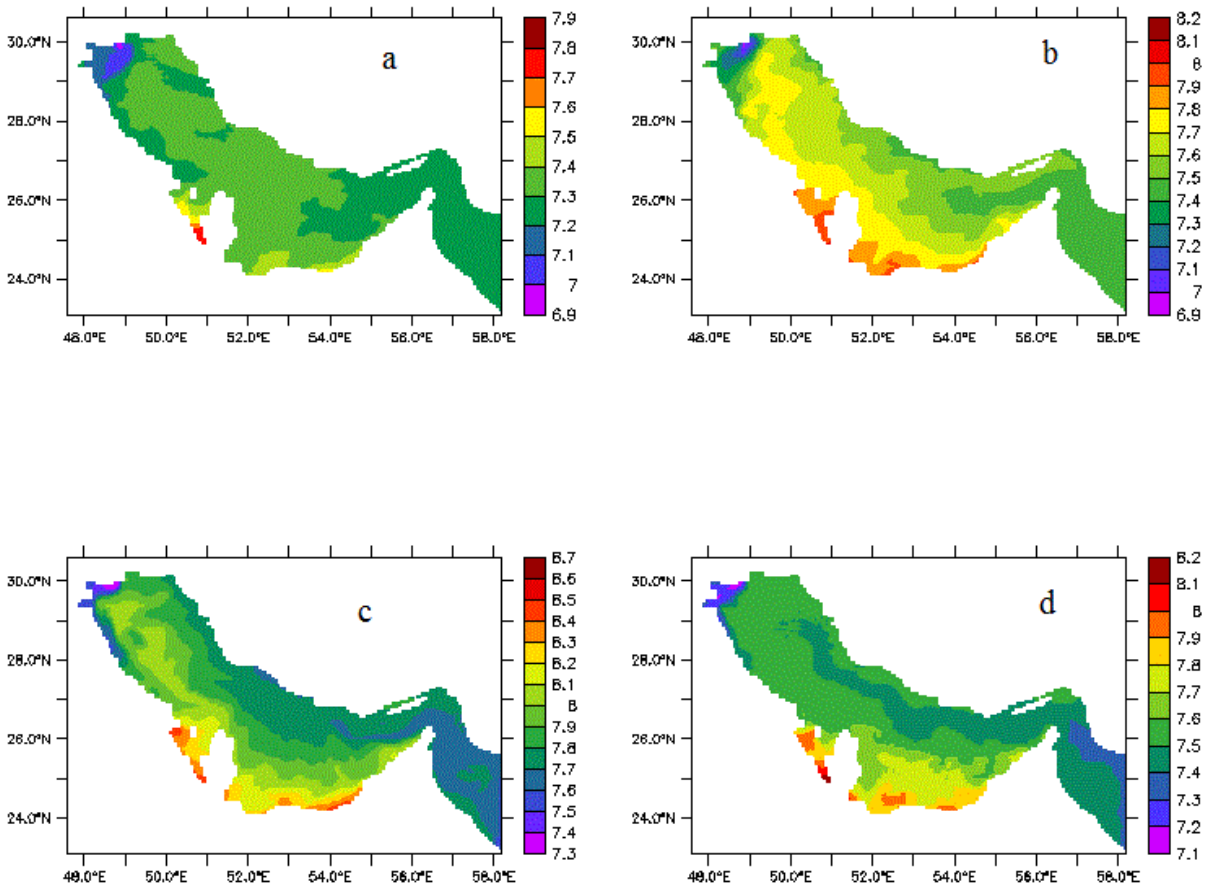


Fig. 10: Spatial distribution real refractive index of surface water of the Persian Gulf n at L-band on (a) January 15, (b) April 15, (c) July 15 and (d) October 15

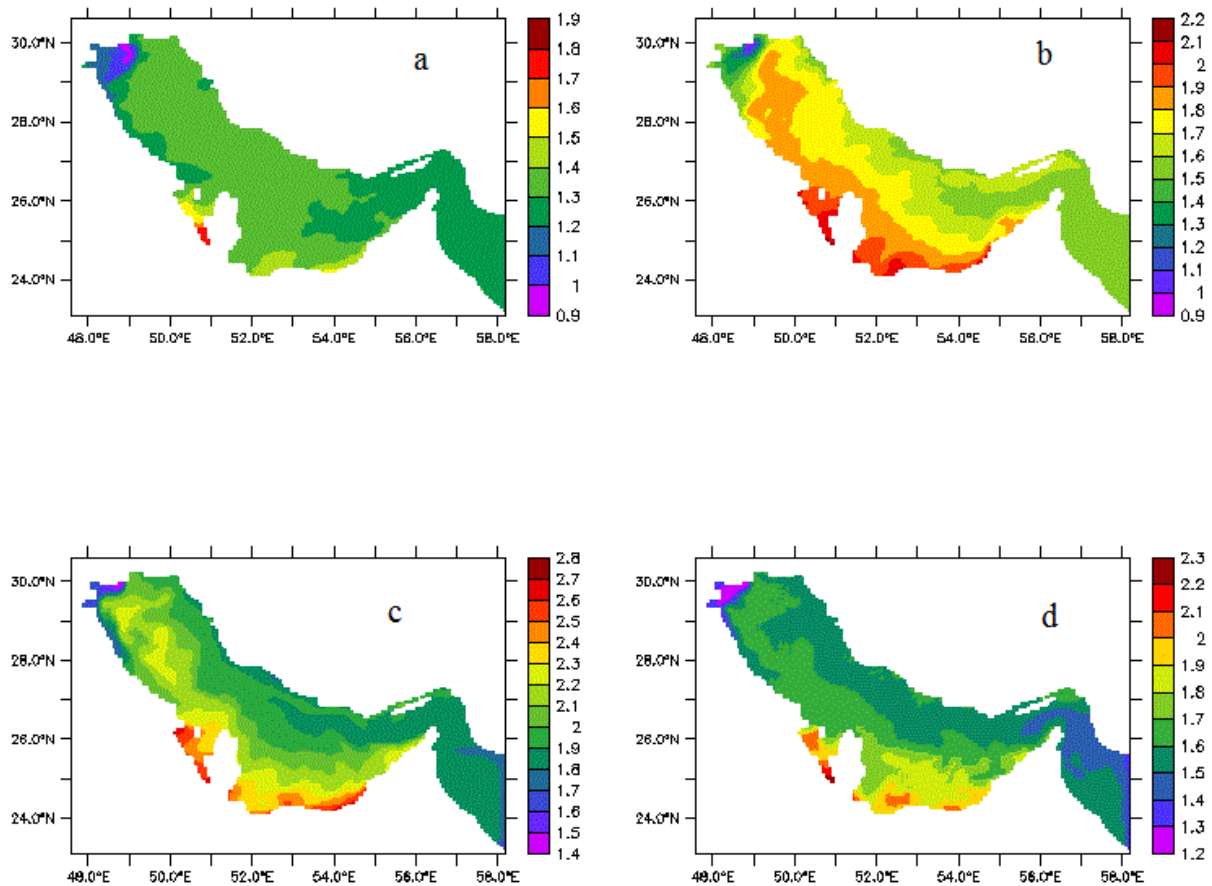


Fig. 11: Spatial distribution the extinction coefficient of surface water of the Persian Gulf  $k$  at L-band on (a) January 15, (b) April 15, (c) July 15 and (d) October 15

Now, with these values of  $n$  and  $k$ , we can calculate the reflectivity of Persian Gulf water for normal incidence at L-band by using equation (18-2). As can be seen from Fig.12, the normal reflectivity in mid-spring varies from 0.823 at the regions close to UAE coast and Bahrain–Qatar shelf to 0.830 in the northwestern end close to Arvand Roud. Furthermore, the reflectivity of water within the Iranian half of Gulf is slightly more than the Southern half close to Arabian countries coasts. Figure 13 shows temporal variability of reflectivity mean over the Gulf. The reflection coefficient mean reaches a maximum value of 0.828 on January and a minimum value of 0.824 on June-August months. In addition, its variability during summer months is very weak. Relatively high value of reflectivity is as a result of high real refractive and low imaginary refractive of the surface water over the Gulf.

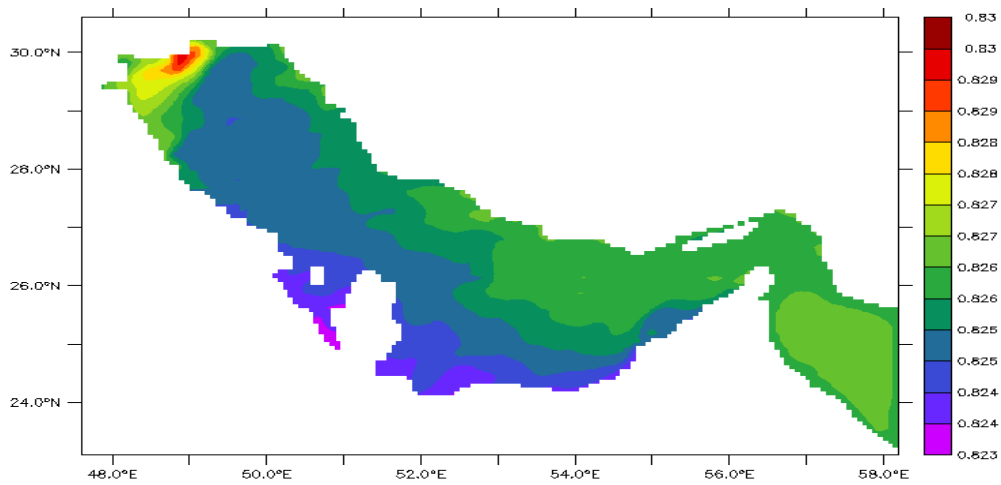


Fig. 12: Spatial variability of reflectivity of Persian Gulf water for normal incidence at L-band on April 15

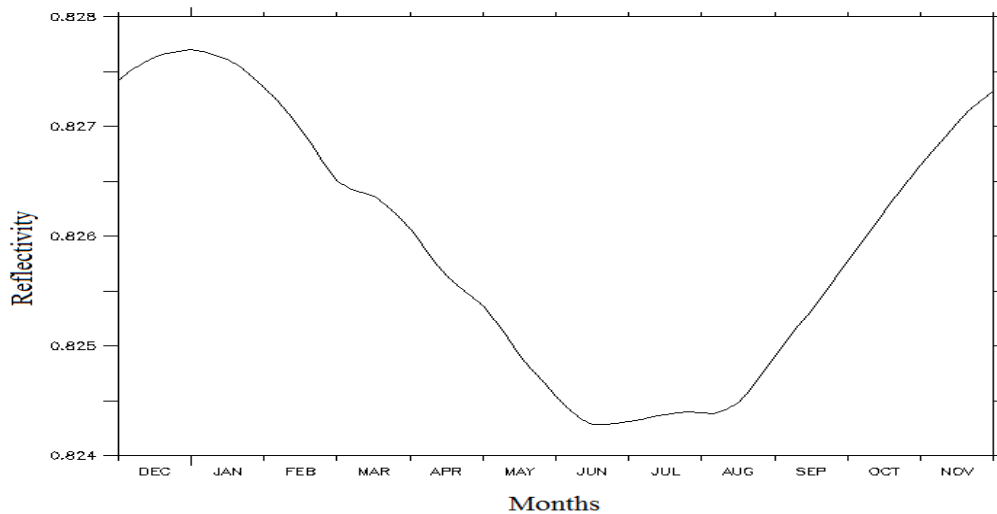


Fig. 13: Time series of domain-averaged reflectivity over the Persian Gulf

#### IV. CONCLUSION

Knowledge of the microwave dielectric Properties of ocean surface is crucial for the measurement of ocean environmental parameters from both spaceborne and airborne microwave radiometers and to understand the properties of radio wave propagation in seawater. Here, at first the complex permittivity was calculated by using Blanch and Aguasca model. All data needed for the model were provided by using a hydrodynamic 3-D numerical model described in our previous papers (Hassanzadeh et al. 2011, Hosseinibalam et al. 2011, Hassanzadeh et al. 2012). Then, permittivity results were used to calculate imaginary and real parts of the refractive index. Finally, these values were employed to estimate reflectivity for normal incidence.

The calculation results indicate that dielectric loss temporal variability of Persian Gulf water is stronger than dielectric constant and it gets maximum values in June-August and minimum values in months of

December-January. The mean dielectric constant  $\epsilon'$  attains a minimum and maximum value during the summer and winter respectively, and varies from 68.18 in June to 71.81 in late January. The dielectric loss  $\epsilon''$  varies from 73.85 in January to 93.44 in June. Contrary to dielectric constant, the dielectric loss decreases from southern shallow parts to northeast deep regions. In winter and autumn due to weak static stability conditions and under the effects of lateral stirring of mesoscale, dielectric properties of Persian Gulf water is more uniform than spring and summer. Totally, temporal variability the complex refractive index and permittivity over shallow regions of Gulf is more than deep regions due to large variations of salinity and temperature. The real refractive index mean over the Gulf surface water varies from minimum value of 7.295 in December to maximum value of 7.875 in June and its annual mean is 7.581 at L-band. The imaginary refractive index mean reach maximum value of 2.036 in June and minimum value of 1/303 in January with

annual mean value of 1.674. The normal reflectivity in mid-spring varies from 0.823 at regions close to UAE coast and Bahrain–Qatar shelf to 0.830 in the northwestern end close to Arvand Roud.

### REFERENCES RÉFÉRENCES REFERENCIAS

1. Blanch, S., and Aguasca, A. (2004), Seawater dielectric permittivity model from measurements at L band, Geoscience and Remote Sensing Symposium, (IGARSS 04): Proceedings Vol 2 (IGARSS, Alaska), 1362-1365.
2. Debye, P. (1929), Polar Molecules, The Chemical Catalog Co., Inc., York, (1929).
3. Ellison, W. J., Balana, A., Delbos, G., Lamkaouchi, K., Eymard, L., Guillou, C., and CPrigent, C. (1998), New permittivity measurements of seawater, *Radio Sci.*, 33.
4. Gadani, D. H., Rana, V. A., Bhatnagar, S. P., Prajapati, A. N. & Vyas, A. D. (2012), Effect of salinity on the dielectric properties of water, *Indian Journal of pure & Applied Physics*, 50, 405-410.
5. Hassanzadeh, S., Hosseinibalam, F., Rezaei-Latifi A. (2011), Numerical modeling of salinity variations due to wind and thermohaline forcing in the Persian Gulf, *Applied Mathematical Modelling*, 35, 1512-1537.
6. Hassanzadeh S., Hosseinibalam, F., Rezaei-Latifi A. (2012), Three-dimensional numerical modeling of the water exchange between the Persian Gulf and Gulf of Oman through the Strait of Hormuz, *Oceanogological and Hydrobiological Studies*, 41, 85-98.
7. Hosseinibalam, F., Hassanzadeh, S., Rezaei-Latifi, A. (2011), Three-dimensional numerical modeling of thermohaline and wind-driven circulations in the Persian Gulf, *Applied Mathematical Modelling*, 35, 5884-5902.
8. John, R. R., Frederick, F. J., Christy, R.W. (2008), *Foundations of Electromagnetic Theory* (4<sup>th</sup> Edition), Paperback - May 19.
9. Joshi, A. S., Deshpande, S. S., Kurtadikar, M. L. (2012), Dielectric Properties of north Indian ocean seawater at 5 GHZ, *International Journal of Advances in Engineering & Technology*, 2, 220-226.
10. Kampf, J., Sadrinasab, M. (2006), The circulation of the Persian Gulf: a numerical study, *Ocean Sci.*, 2, 27-41.
11. Klein, L. A. & Swift, C. T. (1977), "An improved model for the dielectric constant of sea water at microwave frequencies," *IEEE Trans. Ant. Prop.*, vol. AP-25, 104-111.
12. Lang, R. Utku, C., Le Vine, David (2003), "Measurement of the dielectric constant of seawater at L-band", IGARS.
13. Magdalena, D. A., & Peter, W. G. (2012), Dielectric and radiative properties of foam at microwave frequencies: Conceptual Understanding of foam emissivity, *Remote Sens.*, 4, 1162-1189.
14. Meissner, T. and Wentz, F. (2004), The complex dielectric constant of pure and sea water from microwave satellite observations, *IEEE transactions on geosciences and sensing*, 43.
15. Stogryn, A. (1971), "Equations for calculating the dielectric constant of saline water," *IEEE Transactions on Microwave Theory and Techniques*, vol. MIT-19, 733-736.
16. Swift, S. A., Bower, A. S. (2003), Formation and circulation of dense water in the Persian Gulf, *J. Geophys. Res* 108(C1).